Lawrence Berkeley National Laboratory
LBL Publications

Title

Succinonitrile-Lithium Salt Complexes as Solid Catholytes for LLZO-Based Solid-State Batteries

Permalink

Journal

ISSN

Authors

Go, Wooseok
Tucker, Michael C
Doeff, Marca M

Publication Date

DOI

Peer reviewed

Succinonitrile-Lithium Salt Complexes as Solid Catholytes for LLZO-based Solid-State Batteries

Wooseok Go[a], Michael C. Tucker[a,z], Marca M. Doeff[a,z]

[a]Energy Storage and Distributed Resources Division, Lawrence Berkeley National Laboratory,

Berkeley, CA 94720, United States

[z]Corresponding author: mctucker@lbl.gov (M.C. Tucker), mmdoeff@lbl.gov (M.M. Doeff)

Abstract

The thermal and electrochemical properties of several succinonitrile (SN)-based organic ionic plastic crystals (OIPCs) containing lithium bis(trifluoromethanesulfonyl)imide (LiTFSI), lithium bis(oxalate) borate (LiBOB) or mixtures of the two salts, were investigated with the goal of determining which is most promising for use as a catholyte in solid-state lithium batteries. The best combination of properties for this use was found for the mixture containing 3 mol% LiTFSI and 2 mol% LiBOB in SN. Based on these observations, several solid-state cells containing Al-substituted $Li_7La_3Zr_2O_{12}$ separators with composite cathodes consisting of $LiNi_{0.33}Mn_{0.33}Co_{0.33}O_2$ (NMC111), carbon black, and the succinonitrile-salt mixtures were assembled and cycled at room temperature, without exogenous pressure, using a simple design.

Keywords: Plastic crystal, Catholyte; full cell; Solid-state battery; LLZO;

Introduction

All-solid-state batteries (ASSB) show promise as next-generation batteries because of their potential for high energy density and better safety. Variants of LLZO ($Li_7La_3Zr_2O_{12}$) are attractive solid electrolytes for ASSBs due to their high ionic conductivities ($>1\times10^{-4}$ $S \cdot cm^{-1}$ at room temperature) and apparent compatibility with Li metal. However, it is challenging to design cathodes for these cells. To ensure reasonably high areal capacity (which translates into high energy density) for applications such as electric vehicles, cathodes must be in the form of composites, but it is difficult to achieve intimate contact between the active material and the solid electrolyte. Attempts to co-sinter active materials such as NMCs ($LiNi_xMn_yCo_zO_2$; $x+y+z\cong1$) and LLZO together to ensure good contact have met with limited success.[1-3] NMCs and other common cathode materials also undergo volume changes during cycling, which can result in disconnection in the composite cathode and lead to rapid capacity fading. The use of a soft, compliant, solid catholyte between the two solid components in the cell is a possible solution to ensure intimate contact. An ideal solid catholyte must also be ionically conductive, and stable against oxidation ($>$ 4.5 V vs. Li/Li$^+$) but does not need to be stable vs. reduction by lithium metal. Cost, safety, and use of non-critical materials are additional considerations.

Organic Ionic Plastic Crystals (OIPC) are soft and waxy at room temperature. When the OIPC is mixed with one or more lithium salts, the mixtures have excellent lithium ion transport properties and can function as electrolytes in batteries.[4] Succinonitrile (SN, $C_2H_4(CN)_2$) is an OIPC material, and composites of SN with Li salts are reported to have high ionic conductivities ($> 1\times10^{-4}$ $S \cdot cm^{-1}$), good oxidative stability ($>$5 V vs. Li/Li$^+$), and low flammability as well. [4,5] Despite the favorable properties of the SN-Li salt composites, poor chemical stability with Li metal and poor mechanical properties makes them difficult to use alone as solid electrolytes. The polymerization

of nitriles in the SN is catalyzed by Li metal, resulting in fast cell performance degradation.[4] These issues are not concerns if the SN complexes are used as solid catholytes in conjunction with a different solid electrolyte such as LLZO. In that case, a thin dense LLZO layer acts as a separator in the cell, preventing direct contact between the OIPC and metallic lithium. There has been, however, relatively little work to investigate the properties of OIPCs used in this manner, although a recent paper has demonstrated the concept.[6] In this work, we investigated the physical, thermal, and electrochemical properties of several succinonitrile-lithium salt mixtures, focusing on their suitability as solid catholytes in LLZO-based ASSBs. We assembled several cells using the OIPCs with LLZO separators and report on those results here. Figure 1 shows the basic concept of these cells.
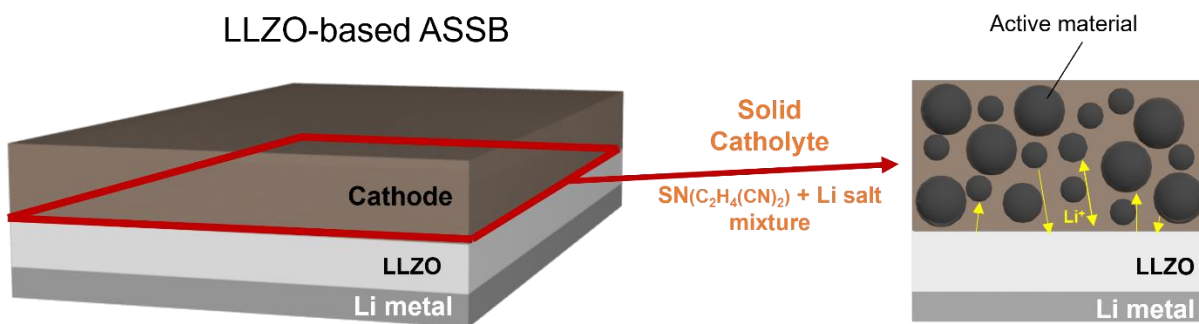

Figure 1. Cell Design. Schematic showing the concept of a cell with dual electrolytes. Dense LLZO is used as the separator. The composite cathode contains active material, PVdF, a carbon additive, and an OIPC consisting of succinonitrile and lithium salts. A gold interlayer is sputtered onto the anode side of the LLZO separator to ensure good adhesion with the lithium anode.

Experimental

Succinonitrile (Sigma-Aldrich, 99 %) and lithium salts of interest were mixed at 80 °C on a hot plate in the desired proportions in an Argon-filled glove box. The Li salts were lithium bis(trifluoromethanesulfonyl)imide (LiTFSI, MSE Supplies, 99.5%) and lithium bis(oxalate)borate (LiBOB, Sigma-Aldrich, 99.9 %). Mixtures were then cooled down to room

temperature. 2032 coin cell (MTI) cases were used for electrochemical property tests. For ionic and electronic conductivity measurements, stainless-steel (SS) plates were used as blocking electrodes. A Teflon washer (thickness 0.78 mm) was placed in between the SS plates in order to fix the volumes of the samples. The mixtures were melted and transferred into the Teflon washer, then cooled down to room temperature to solidify them. The ionic conductivities of the Li salt-SN mixtures were then measured at room temperature using Electrochemical impedance spectroscopy (EIS) with a Bio-Logic VSP-300, over a frequency range of 0.1 Hz to 7MHz. The electronic conductivity was measured using direct current (DC) polarization with an applied potential of 0.5 V for 1 hour. The cells for the linear sweep voltammetry (LSV) experiments were composed of Li metal reference electrodes and stainless-steel plates as counter electrodes using thin LLZO films. The applied voltage range was from 3.0 to 5.5 V vs. Li/Li^+ with a scanning speed of 1 mV/sec. The molten Li salt-SN mixtures were dropped onto solid LLZO sheets, and the droplet was observed using a digital camera with a holder in an Argon gas filled glove box at 80 ℃. Contact angles were measured using an image analysis program (imageJ). Their thermal behavior was observed using an optical microscope (BA310Met, Motic) and measured by differential scanning calorimetry (DSC, PerkinElmer, DSC 8000) over a temperature range of -80 to 80 ℃ at a rate of 10 ℃/min under Ar atmosphere.

Polycrystalline $LiNi_{0.33}Mn_{0.33}Co_{0.33}O_2$ (NMC, Ampcera, MSE) was used as the active cathode material for the solid-state cells. Carbon black (Acetylene black, DENKA) was used as the electronically conductive additive, Polyvinylidene fluoride (PVdF, Sigma-Aldrich) as a binder, and the Li salt-SN mixture as the solid catholyte. A slurry in NMP (N-methyl-2 pyrrolidone) was prepared using NMC, carbon black, and PVdF binder in the weight ratio of 8:1:1 and was cast on

carbon-coated Al foil to make the cathodes. The electrode was dried in vacuum chamber at 150°C for 12 hours. The cathode loading was 1.5 mg/cm^2 (active material: 1.2 mg/cm^2).

LLZO dense layers were prepared using a tape casting method.[7, 8] Al-substituted LLZO powder (Li$_{6.25}$Al$_{0.25}$La$_3$Zr$_2$O$_{12}$, 500 nm, MSE Supplies), MgO (50 nm, US Research Nanomaterials Inc.), Li$_2$CO$_3$ (Sigma-Aldrich >99.0 %), and dispersant (DS002, Polymer Innovations) were mixed in toluene solvent. The slurry was then ball milled using ZrO$_2$ balls (2 mm diameter) and a planetary ball milling machine (500 rpm, 30 min, PM200, Retsch). An organic binder (MSB-1-13, Polymer Innovations Inc.) was added to the solution and mixed for 3 hours. Tape casting was conducted using Silicon-coated Polyethylene terephthalate (PET) film as a carrier substrate. The doctor blade gap for the tape casting was set to 200 μm. The prepared tapes were dried overnight, then detached from the substrate. After cutting the tapes into appropriate shapes, several tapes were stacked and laminated at a temperature of 90°C and pressure of 20 MPa for 10 min. Prior to sintering, the laminated films were heated at 675°C under ambient air conditions to burn out the binder. Afterward, the films were sintered between carbon papers (Panasonic) to prevent interaction with the Al$_2$O$_3$ substrate. A tube furnace with Ar flowing atmosphere (200 mL/min) was used for sintering. The sintering was conducted at 1100 °C for 4 hours with a heating rate of 2°C/min.

Symmetric Li salt-SN mixture cells were prepared using thin LLZO as electrolyte. The Li salt-SN mixtures were melted at 80°C and drop-casted on both side of the LLZO. Stainless steel plates were used as a current collector for both sides. The prepared cells were tested in a temperature controlled chamber at 25°C.

LLZO-based solid-state cells were fabricated in an Ar-filled glove box. On the anode side, Au was sputtered (108 Auto, Cressington sputter) on the LLZO surface, then Li metal was melted on the Au sputtered surface to form intimate contact. On the cathode side, the Li salt-SN mixture

was melted at 80ºC and drop-casted onto the LLZO, which was pre-heated to 80ºC, then the composite cathode was placed on top of the mixture. Conventional 2032 coin cell cases (MTI) with crimpers were used for cell assembly. Instead of a conventional metallic spring, carbon felt was used to avoid excessive pressure on the thin LLZO electrolyte. The solid-state cells were cycled using an Arbin cycler (LBT21084). During cycling, the cells were placed in a temperature-controlled oven at 25ºC. The cells were cycled between 3.0 and 4.3 V range at 0.1 C-rate, equivalent to a current density of 18.0 $\mu A/cm^2$. C-rate is defined as the current needed to discharge the cell fully in one hour, assuming a cathode capacity of 150 mAh/g.

Results and Discussion

The properties of various Li salt-SN mixtures, including thermal behavior, oxidative stability, conductivity, wetting on LLZO, and chemical stability against LLZO were characterized using ex-situ and electrochemical methods. A dual-salt composition was selected as the most promising, and its use as a catholyte was demonstrated in a full cell.

Several mixtures of succinonitrile with either LiTFSI or LiBOB were prepared as described in the Experimental Section and as shown in Figure 2a. Up to 15 mol% LiTFSI could be incorporated into the SN, although at or above 7.5 mol%, the mixtures were liquid at room temperature, presumably due to melting point suppression by the salt (Figure S1a). LiBOB was much less soluble with a limit of 3 mol% (Figure S1b).[9] Mixtures containing both LiTFSI and LiBOB in different proportions were also prepared (Figure S1c). Figure 2b-d shows optical images of the three types of Li salt-SN mixtures: 5 mol% LiTFSI, 3 mol% LiBOB, and dual salt (3 mol% LiTFSI+ 2 mol% LiBOB). These images show that the mixtures consist of randomly oriented domains, which exhibit seaweed growth patterns, known as the signature of SN plastic crystals.[10]
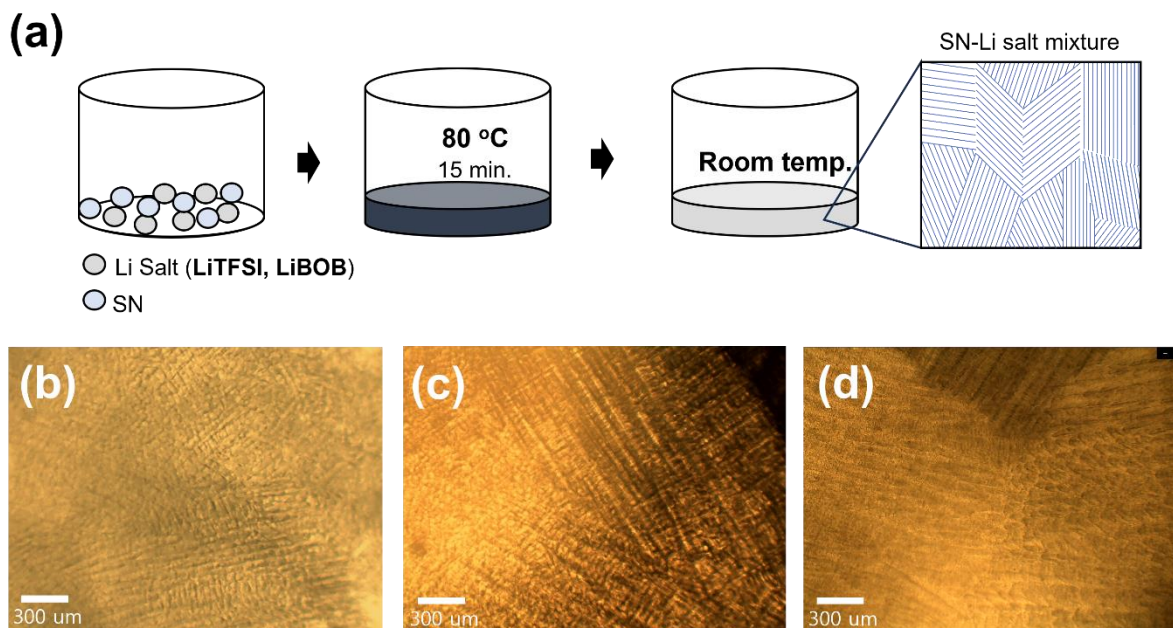
Figure 2. Preparation and crystallization of mixtures. (a) Schematic of preparation of the Li-salt-SN mixtures and (b-d) optical images of LiX-SN organic ionic plastic crystals. (b) 5 mol% LiTFSI. (c) 3 mol% LiBOB. (d) Dual salt (3 mol% LiTFSI + 2 mol% LiBOB).

The thermal behavior of the single-salt systems was observed using DSC in the temperature range of -80 to 80°C (Figure 3), and in all cases the mixtures are solid at room temperature. Pure succinonitrile melts at 57°C[4], LiTFSI at 234°C[11], and LiBOB at 300°C. [12] In the LiTFSI systems, two endothermic peaks were observed (Figure 3a) for most of the samples. The peaks at lower temperatures correspond to the crystal to plastic crystal transition (T_{pc}), and the higher temperature peak to melting (T_m). [4, 13] When the LiTFSI content was increased from 1 to 7 mol%, Tpc values were almost constant (-36.3°C), but the T_m decreased significantly from 39.0 to 29.7°C. Melting point depression of plastic crystals is also observed in similar systems. [10, 13] The melting point depression means that the LiTFSI-SN system is a solid at room temperature only up to about 5 mol% LiTFSI. In the LiBOB-SN system (Figure 3b), T_{pc} is almost constant (-36.2°C) with salt concentration and the depression of T_m also dependent on salt concentration, with a value of 48.2°C

for 3 mol% LiBOB. However, some of the LiBOB-SN samples show two thermal transitions at elevated temperatures (for example, for the 1 mol% LiBOB mixture there are two close peaks at 46.8 and 55.6^{o}C). One possible explanation is that two phases co-exist in this temperature range, one that is LiBOB-rich, which melts at 46.8^{o}C, and another that is LiBOB-poor, which melts at 55.6^{o}C. When the LiBOB content was increased to 2 mol%, the two close peaks combined into one broad peak located at 48.9^{o}C. At 3 mol%, only one somewhat less broad melting peak at 48.2^{o}C was observed, possibly indicating that the phases are integrated into one. Data was also obtained for the 5 mol% LiBOB system, even though this exceeds the solubility limit at room temperature. Results are similar to those obtained for 3 mol % LiBOB indicating that the presence of undissolved LiBOB does not change the thermal properties. The thermal behavior of the dual salt systems is shown in Figure 3c. For all dual-salt mixtures, three endothermic peaks were observed. The lowest temperature crystal to plastic crystal transition peaks (T_{pc}) were at -36.4^{o}C and almost constant for the dual-salt mixtures. All single and dual salt mixtures in this study had very close values of T_{pc}, which indicates it is independent of Li salt. At the higher temperature range, two peaks were observed. The higher temperature peak corresponds to T_m and the melting of the mixture was clearly observed visually. We speculate that the lower temperature peak corresponds to partial melting of the plastic crystal, implying that the liquid and plastic crystal phases coexist in the temperature range between the two peaks. From these data, a phase diagram was constructed (Figure 3d). Here, the x-axis indicates the Li salt ratio of LiTFSI/(LiTFSI+LiBOB) where the total salt concentration was maintained at 5 mol%. The salt mixtures were completely soluble in SN at the ratios indicated in the graph. All the mixtures also show two melting transitions (Figure 3c) indicating partial melting in the indicated temperature range.
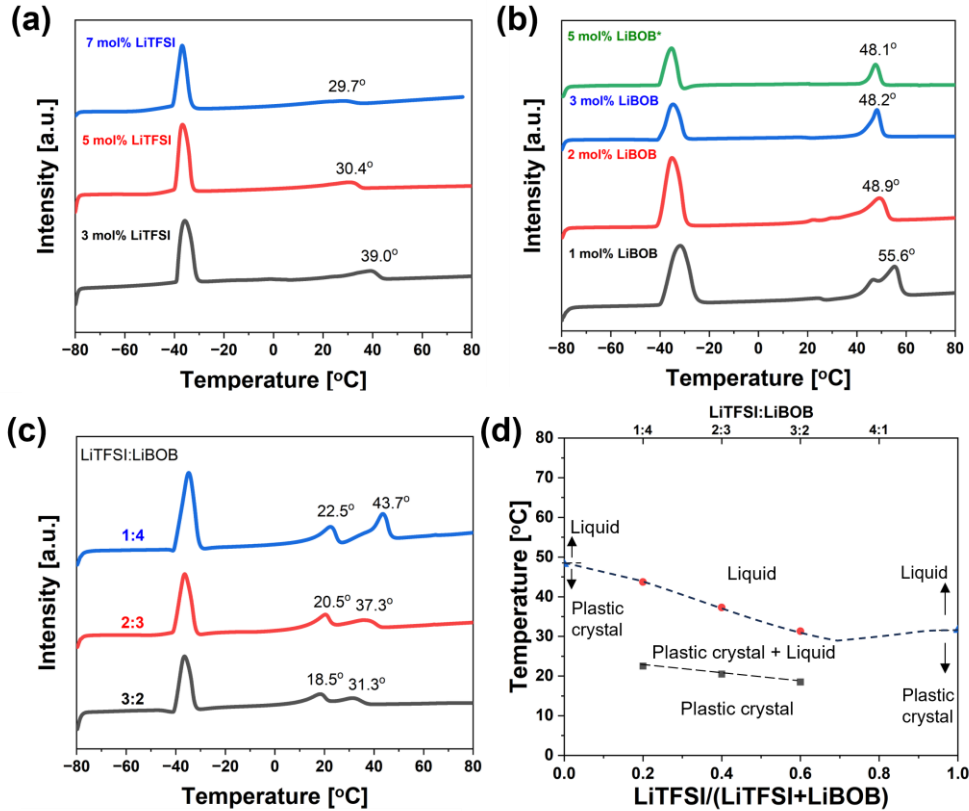
Figure 3. Thermal behavior of SN-Li salt mixtures. (a-c) DSC data for the SN-Li salt mixtures (a) SN-LiTFSI mixture, (b) SN-LiBOB mixture, and (c) Dual-salt mixture. For the mixtures, the total salt content was held at 5 mol%. Note that for the SN-LiBOB mixtures, 5 mol % LiBOB exceeds the solubility limit at room temperature. (d) Phases of SN/LiBOB/LiTFSI mixtures determined by DSC measurements. Total amount of dissolved salt is 5 mol%.

The variation of melting temperature with salt type and salt concentration has implications for the operation of cells containing the OIPCs. Unlike LLZO and other ceramic conductors, Li salt-SN systems are dual ion conductors; i.e., both cations and anions are mobile. In this regard, they resemble liquid or polymeric electrolytic solutions, which are highly non-ideal. In those systems, cationic transference numbers are usually less than 1, and can even be negative, [14, 15] indicating high mobility of negatively charged triplets or aggregates compared to single cations. This leads to the development of concentration gradients throughout the cell when current is passed. In extreme cases, depletion or precipitation of salts can occur, leading to cell failure. [14, 15] Proper

design of cells (e.g., optimized component thicknesses) can mitigate this. However, in the case of cells containing the Li salt-SN systems, the variation in salt concentration may also result in changes in the melting temperature. It is not inconceivable that a high concentration of LiTFSI, for example, in a polarized cell would cause localized melting even at room temperature. Carbon and active material particulates, however, provide nucleation sites for rapid re-freezing once the concentration gradients relax. The thermal properties not only can provide a self-healing mechanism but ensure good contact among cell components during operation in spite of the volume changes, without the catholyte completely melting. Cells can be designed with this in mind, although future detailed thermal studies of operating cells would be fruitful.

Ionic conductivities of the solid single-phase mixtures were measured using EIS. The values were determined from the intercepts of the high frequency semi-circles with the real axes in the Nyquist plots as shown in Figures S2 and 4a and given in Table 1. The ionic conductivity of the 5 mol% LiTFSI-SN was an order of magnitude higher than that of 3 mol% LiBOB-SN. For the dual-salt mixtures, the conductivities fell in between the single-salt mixtures, but with acceptable room temperature conductivities of $> 1 \times 10^{-3}$ $S \cdot cm^{-1}$ (Figure S2). As the LiTFSI content decreased in the dual-salt mixture, so did the conductivity. The dual-salt mixture containing 3 mol% LiTFSI and 2 mol% LiBOB had an ionic conductivity of 2.64×10^{-3} $S \cdot cm^{-1}$. This composition was selected as the best compromise between the electrochemical and thermal properties, and was used for further studies and cell operation, below.
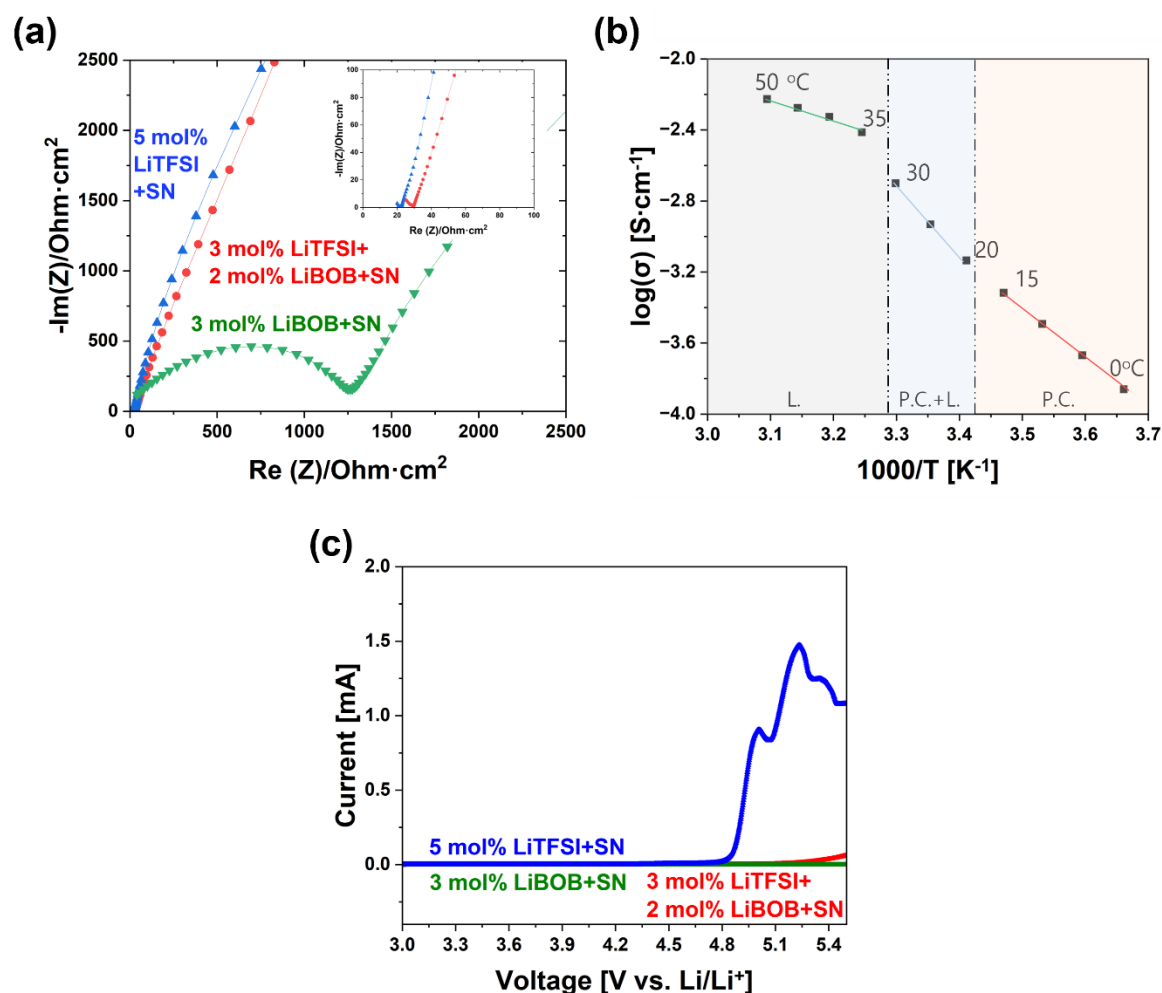
Figure 4. Electrochemical characterization. (a) EIS and (c) LSV of selected Li salt-SN catholytes at RT. (b) Arrhenius plot of a dual-salt mixture (3 mol% LiTFSI, 2 mol% LiBOB) in the temperature range of ~0-50°C. P.C.= Plastic crystal, L= Liquid.

Table 1. Electrochemical properties of SN salt mixtures.

	5 mol% LiTFSI	3 mol% LiBOB	Dual salt (4:1)[a]	Dual salt (3:2)[a]	Dual salt (2:3)[a]	Dual salt (1:4)[a]
$\sigma_{RT, ionic}$, **S·cm⁻¹**	3.46×10^{-3}	5.58×10^{-5}	3.41×10^{-3}	2.64×10^{-3}	1.87×10^{-3}	1.28×10^{-3}
Oxidative stability limit, **V**[b]	4.7	> 5.5	4.9	5.0	5.1	5.3
$\sigma_{RT, electronic}$, **S·cm⁻¹**	1.26×10^{-9}	3.79×10^{-9}	5.63×10^{-9}	4.72×10^{-9}	9.75×10^{-9}	1.40×10^{-8}

a) Ratios of LiTFSI and LiBOB in mol%
b) Determined when current reached a value of 1 $\mu A/cm^2$.

Ionic conductivities of the dual-salt mixture were also measured in the temperature range of 0 to 50 °C and plotted in Figure 4b. As temperature increased, higher conductivities were observed (Figure S3). The mixture showed 1.4×10^{-4} $S \cdot cm^{-1}$ at 0°C, and 5.9×10^{-3} $S \cdot cm^{-1}$ at 50°C. The plot shows three distinct temperature regions corresponding to the thermal events identified in Figure 3c, and the activation energy in each region was estimated. The activation energies were 0.56 eV in the low temperature region (0 to 18.5 °C) where the mixture is a solid plastic crystal, 0.77 eV at intermediate temperatures (18.5 to 31.3 °C), and 0.24 eV in the high temperature region (31.3 to 50 °C) where the mixture is completely liquid. These values are within the range reported for similar plastic crystal materials based on succinonitrile (0.14 to 0.77 eV, Table S1). Electronic conductivities of the mixtures were also measured (Figure S4) using DC polarization and are given in Table 1. All the mixtures showed electronic conductivities on the order of 10^{-9} $S \cdot cm^{-1}$, confirming that they are electronic insulators.

The oxidative stability of the single salt SN and the dual salt SN (3 mol% LiTFSI and 2 mol% LiBOB) mixtures were examined using Linear Sweep Voltammetry (LSV) as shown in Figure 4b. The 5 mol% LiTFSI-SN exhibited significant current flowing above 4.7 V due to LiTFSI salt decomposition. Despite the reduced oxidative stability, LiTFSI-SN should still be compatible with most cathode active materials such as NMCs, which are typically charged to 4.2-4.3 V vs. Li/Li$^+$. The LiBOB-SN mixture exhibited negligible current below 5.5 V implying that the LiBOB-SN mixture has better oxidative stability than the one with LiTFSI, consistent with the high oxidative stability of the LiBOB. [16] The dual salt-SN mixture has an oxidative limit of ~4.8-5.3 V, intermediate between that of LiTFSI-SN and LiBOB-SN. This implies that the LiBOB salt retards

oxidation of the LiTFSI salt in the mixture. Enhanced oxidative stability by adding LiBOB into an LiTFSI-containing polymer electrolyte has also been previously observed. [17]

The wettability of Li salt-SN mixtures on thin LLZO sheets is shown in Figure 5a-c. All three mixtures have contact angles of less than 90° indicating fairly good wettability on LLZO. This suggests that the Li salt-SN mixture can fill open pores in LLZO dense layers and form intimate contact, and may be melt-infiltrated easily into porous LLZO scaffolds.
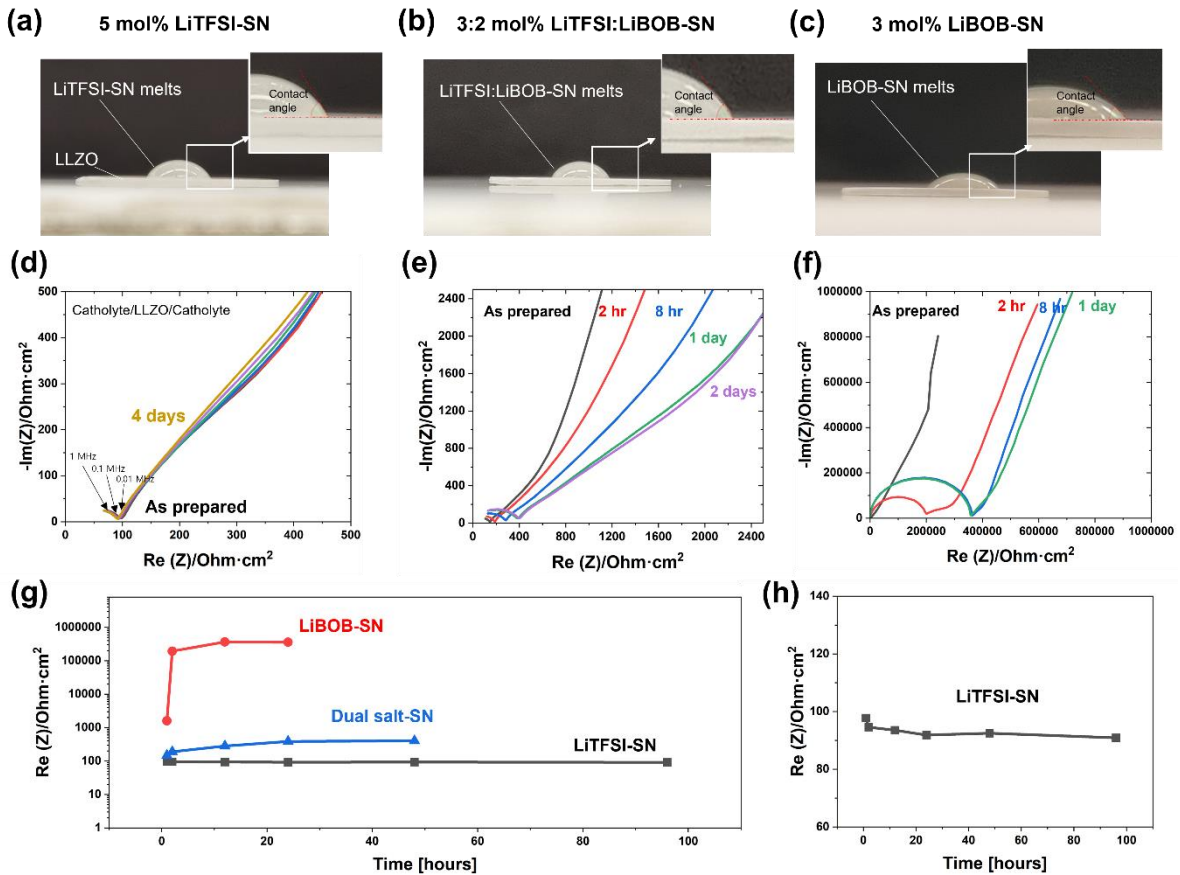
Figure 5. Wetting and stability in contact with LLZO. (a-c) Contact angle measurements of molten Li salt-SN mixtures on dense LLZO, (d-f) Nyquist plots showing changes in symmetrical cell impedance for (d) 5 mol% LiTFSI-SN (e) 2 mol% LiBOB+3 mol% LiTFSI-SN and (f) 3 mol% LiBOB-SN, (g-h) Time dependance impedance evolution of the symmetric cells for (g) three kinds of mixtures (h) LiTFSI-SN only.

In order to determine the chemical stability of Li salt-SN mixtures with the LLZO electrolyte, symmetric cells with SN mixtures on both side of LLZO were prepared (Figure S5a), and time-dependent impedance evolution was evaluated at 25°C as shown in Figure 5d-h. The EIS plot of the as-prepared LiTFSI-SN symmetric cell (Figure 5d) shows a semicircle in the high frequency range and a sloping line in the low frequency range. The semicircle at high frequency (1~0.01 MHz) corresponds to the LLZO electrolyte and Li salt-SN mixture as shown in Figure S5c-d. In the mid-frequency range, there was no additional feature, indicating that the interface resistance between the LLZO and Li salt-SN mixture is very small. The suggested equivalent circuit and fitting result are shown in Figure S5b and S5e. Up to 4 days of storage, there was no noticeable change in the EIS plot, showing evidence of very little chemical reactivity between the LLZO and LiTFSI-SN mixture. In contrast, LiBOB-SN shows significant changes after 1 day as shown in Figure 5f. The semicircle increased in size ~1,000 times in 2 hours, and the increase saturated after 8 hours with an areal resistance of ~350,000 ohm·cm^2. The dual salt-SN cell (Figure 5e) showed similar behavior to the cell with LiBOB-SN, but to a much lesser extent. The resistance increased 2.8 times after 1 day but stabilized after this time. The reason for this smaller resistance increase can be attributed to the smaller amount of LiBOB salt.

The electrochemical performance of LLZO-based solid-state cells using two different Li salt-SN mixtures as catholyte are shown in Figure 6. The cells consist of Li metal anodes, thin LLZO electrolytes (thickness of 80 μm), melt infiltrated Li salt-SN mixture, and the composite NMC111 cathode. The interface between LLZO and cathode is shown in Figure 6a. Because the catholyte was filling the space between the NMC111 and the LLZO, no pores were observed at the interface indicating an intimate contact. The interface between the NMC111 and catholyte is also shown in

Figure 6b, and the catholyte was filling the space between the NMC particles as well. Note that the cells were cycled at 25°C without exogeneous pressure.
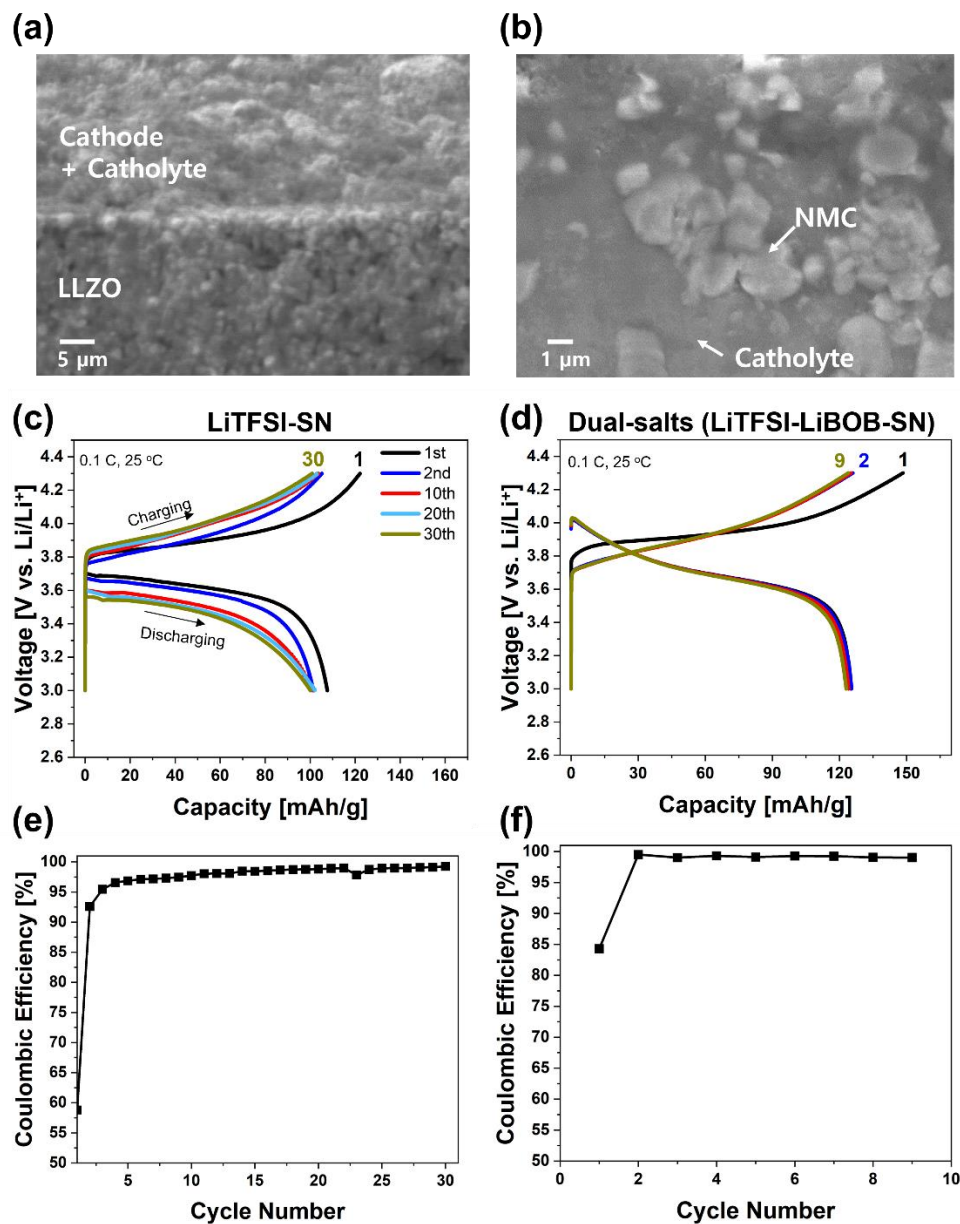
(a)

(b)

(c) LiTFSI-SN

(d) Dual-salts (LiTFSI-LiBOB-SN)

(e)

(f)

Figure 6. Full cell demonstration. SEM observation on the interface between (a) LLZO and cathode, and (b) interface in the composite cathode. Galvanostatic charge/discharge curve for Li/LLZO/NMC cell using (c) LiTFSI-SN mixture as catholyte and (d) dual salt-SN mixture as catholyte. Coulombic efficiency of the (e) LiTFSI-SN cell and (f) dual salt-SN cell. The cells were tested at 0.1 C-rate in the 3.0 to 4.3 V range at 25°C with no external pressure.

A cell with the LiBOB-SN mixture could not be cycled, most likely because of the high reactivity and the lower ionic conductivity of this catholyte. The performance of a solid-state cell using the LiTFSI-SN mixture is shown in Figure 6c-f. During the first cycle, it delivered 125 mAh/g upon charge and 110 mAh/g upon discharge. This first cycle irreversibility is typical behavior for NMC cathodes and has been attributed to the slow kinetics of lithium re-insertion near the end of discharge. [18] After that, the cell retained a capacity of ~105 mAh/g with good reversibility for 30 cycles (Figure 6e), indicating that the mixture is working properly as a catholyte. However, the voltage difference between charge and discharge increased upon cycling, suggesting impedance rise.   When the dual salt-SN mixture was used as a catholyte, higher capacity and more stable cycling performance was achieved, as shown in Figure 6d. The first cycle charge capacity was 148 mAh/g and the following discharges were about 125 mAh/g, somewhat lower than the theoretical value, but with good capacity retention (Figure 6f). The higher capacity than the LiFSI-SN cell is due to the lower impedance as shown in the Figure S6a-b. During this cycling, the voltage profile showed little change, indicating that the dual-salt mixture works better than either of the single salt mixtures. Enhanced cycling performance in dual salt (LiTFSI and LiBOB) systems in polymer [19] and liquid [20-22] electrolytes has also been reported in other studies and can be attributed to formation of a stable cathode-electrolyte interface (CEI) layer formed by LiBOB on cathode surfaces. [22]

Conclusions

We studied Li salt-SN mixtures for use as solid-catholyte in LLZO-based solid-state cells. Using LiTFSI and LiBOB as Li salts mixed with SN, single-salt and dual-salt mixtures were prepared, and their properties were compared to determine the best mixture to use in a solid-state

cell. The dual-salt mixture containing 3 mol% LiTFSI and 2 mol% LiBOB in SN showed the best compromise of properties including ionic conductivity of 2.64×10^{-3} S·cm^{-1}, oxidative stability up to 5.0 V, and fair chemical stability with LLZO. Using this mixture, a solid-state cell containing NMC111 was cycled stably and delivered a capacity of ~125 mAh/g. The findings demonstrated that the dual salt-SN mixture is a superior SN-based catholyte to use in a solid-state cell with a LLZO separator.

References

1. M. Ihrig, M. Finsterbusch, A. M. Laptev, C. H. Tu, N. T. T. Tran, C. A. Lin, L. Y. Kuo, R. Ye, Y. J. Sohn, P. Kaghazchi, S. K. Lin, D. Fattakhova-Rohlfing, and O. Guillon, *ACS Appl Mater Interfaces,* **14** (9), 11288-11299 (2022).
2. Y. Ren, T. Liu, Y. Shen, Y. Lin, and C.-W. Nan, *Journal of Materiomics,* **2** (3), 256-264 (2016).
3. L. Miara, A. Windmuller, C. L. Tsai, W. D. Richards, Q. Ma, S. Uhlenbruck, O. Guillon, and G. Ceder, *ACS Appl Mater Interfaces,* **8** (40), 26842-26850 (2016).
4. P. J. Alarco, Y. Abu-Lebdeh, A. Abouimrane, and M. Armand, *Nat Mater,* **3** (7), 476-481 (2004).
5. Q. Zhang, K. Liu, F. Ding, W. Li, X. Liu, and J. Zhang, *ACS Appl Mater Interfaces,* **9** (35), 29820-29828 (2017).
6. H. Shen, E. Yi, S. Heywood, D. Y. Parkinson, G. Chen, N. Tamura, S. Sofie, K. Chen, and M. M. Doeff, *ACS Appl Mater Interfaces,* **12** (3), 3494-3501 (2020).
7. R. A. Jonson, E. Yi, F. Shen, and M. C. Tucker, *Energy & Fuels,* **35** (10), 8982-8990 (2021).
8. R. A. Jonson and P. J. McGinn, *Solid State Ionics,* **323** 49-55 (2018).
9. A. Abouimranez and I. J. Davidson, *Journal of The Electrochemical Society,* **154** (11), 1031 (2007).
10. M. Echeverri, N. Kim, and T. Kyu, *Macromolecules,* **45** (15), 6068-6077 (2012).
11. M. J. Marczewski, B. Stanje, I. Hanzu, M. Wilkening, and P. Johansson, *Phys Chem Chem Phys,* **16** (24), 12341-12349 (2014).
12. E. Zinigrad, L. Larush-Asraf, G. Salitra, M. Sprecher, and D. Aurbach, *Thermochimica Acta,* **457** (1-2), 64-69 (2007).
13. W. Zha, J. Li, W. Li, C. Sun, and Z. Wen, *Chemical Engineering Journal,* **406** (2021).
14. M. M. Doeff, A. Ferry, Y. Ma, L. Ding, and L. C. D. Jonghe, *Journal of The Electrochemical Society,* **144** L20 (1997).
15. Y. Ma, M. Doyle, T. F. Fuller, M. M. Doeff, L. C. D. Jonghe, and J. Newman, *Journal of The Electrochemical Society,* **142** 1859 (1995).
16. Y. Wang, L. Xing, X. Tang, X. Li, W. Li, B. Li, W. Huang, H. Zhou, and X. Li, *RSC Adv.,* **4** (63), 33301-33306 (2014).
17. S. Li, Y.-M. Chen, W. Liang, Y. Shao, K. Liu, Z. Nikolov, and Y. Zhu, *Joule,* **2** (9), 1838-1856 (2018).
18. S.-H. Kang, D. P. Abraham, W.-S. Yoon, K.-W. Nam, and X.-Q. Yang, *Electrochimica Acta,* **54** (2), 684-689 (2008).
19. X. Lin, J. Yu, M. B. Effat, G. Zhou, M. J. Robson, S. C. T. Kwok, H. Li, S. Zhan, Y. Shang, and F. Ciucci, *Advanced Functional Materials,* **31** (17), 2010261 (2021).
20. S. Jiao, X. Ren, R. Cao, M. H. Engelhard, Y. Liu, D. Hu, D. Mei, J. Zheng, W. Zhao, Q. Li, N. Liu, B. D. Adams, C. Ma, J. Liu, J.-G. Zhang, and W. Xu, *Nature Energy,* **3** (9), 739-746 (2018).
21. J. Zheng, M. H. Engelhard, D. Mei, S. Jiao, B. J. Polzin, J.-G. Zhang, and W. Xu, *Nature Energy,* **2** (3), (2017).
22. M. Song, C. Tian, C. Chen, T. Huang, and A. Yu, *Journal of Power Sources,* **567** (2023).